18th International Conference on Information Fusion
Washington, DC - July 6-9, 2015

Filter Initialization and Batch Estimation for Tracking with Angular-Only Measurements

Dietrich Fränken
Sensor Tracking
Airbus Defence & Space
D-89077 Ulm, Germany
Email: dietrich.fraenken@airbus.com

***Abstract*—The task of tracking objects with angular-only measurements imposes an interesting estimation problem due to the fact that range information is not obtainable when the sensor is mounted on a non-maneuvering platform and the tracked object itself is moving as well. Here, the use of log-spherical state variables within an extended Kalman filter is a well-established approach to tackle the problem. This paper focusses on the initialization of such a filter. A suitable (approximate) prior for the non-observed quantities is derived aiming for an initialization with a single measurement pair of bearing and elevation. Alternatively, filter initialization can be performed by applying a batch estimator using several such measurement pairs. One possible estimator of this kind is also presented. Simulation results using both schemes are provided.**

I. Introduction

The problem of tracking with angular-only measurements is widely discussed in literature and may appear in context with a lot of different applications. One such application is that of tracking with measurements from jammed radar (cf. [1], [2] and the reference cited therein), another one is the use of optical sensors for collision avoidance and separation of manned or unmanned air traffic participants (see, e. g., [3]–[5]). A well-established tracking approach for the problem is based on a state space in modified polar coordinates as been introduced in [6] with the refinement of using log-polar coordinates as proposed (for 2D) in [7]. But, while there is improved tracking performance using those coordinates within an *extended Kalman filter* (EKF), "accurate initialisation is crucial to obtaining effective tracking performance for the single sensor bearings-only problem" according to that very same paper. However, the initiation scheme proposed by the authors starts from measurements being converted to Cartesian space (with some chosen default range) and thus does not operate in log-spherical space directly. With this paper, we try to fill, at least to some extent, that gap that also has been left open in our previous related publication [8]. Herein, we will discuss the 3D case based on log-sperical coordinates. The reduced 2D case in log-polar coordinates is implicitly covered by this as well. It should be mentioned at this point that more advanced non-linear estimation techniques like the unscented Kalman filter [9] or the particle filter [10] may also be applied to the investigated tracking problem, but this is beyond the scope of this paper.

We will start our discussion by shortly recalling the fundamental properties of log-spherical coordinates as well as propagation and update of an EKF based thereon where we follow our presentation in [8]. Afterwards, we will derive a suitable prior for the quantities not observed when initialization is based on one measurement pair. We will see that this prior is exact for a non-moving platform only, but we will somewhat heuristically apply it in adapted form for moving platforms, too. As an alternative to that one-point initialization, we will investigate a regression-based batch estimator using multiple measurement pairs for track initialization. For Cartesian-complete measurements, one minimal example for such an estimator is known as two-point differencing [11] (with an exact solution to the resulting system of equations), but multiple-point initialization with a weighted least-squares solution to an over-determined system of (linear) equations is common practice there as well which motivated us to search for an analogeous initialization scheme in the case of angular-only measurements. Simulation results conclude this paper.

II. Log-Spherical Coordinates

For the sake of conciseness, we assume a constant velocity motion model for the platform and an (ideally undisturbed) motion model of the same type for the object to be tracked. In the following presentations, positions as well as their polar representations (ranges and angles) are considered in a Cartesian coordinate system with constant orientation, e. g., an east-north-up (ENU) system centered within and moving with the ownship position. Velocities and log-spherical rates are relative to the moving platform and referenced in the same coordinate system.

We use the (relative) bearing angle β and the (relative) elevation angle ε following the convention

$$\begin{aligned} x &= r\cos\beta\cos\varepsilon \\ y &= r\sin\beta\cos\varepsilon \\ z &= r\sin\varepsilon \end{aligned} \tag{1}$$

With the unitary rotation matrices

$$\mathbf{B}(\beta) = \begin{bmatrix} \cos\beta & -\sin\beta & 0 \\ \sin\beta & \cos\beta & 0 \\ 0 & 0 & 1 \end{bmatrix} \tag{2}$$

and

$$\mathbf{E}(\varepsilon) = \begin{bmatrix} \cos\varepsilon & 0 & -\sin\varepsilon \\ 0 & 1 & 0 \\ \sin\varepsilon & 0 & \cos\varepsilon \end{bmatrix} \tag{3}$$

the position $\mathbf{p} = [x, y, z]^T$ following eq. (1) can be written as

$$\mathbf{p} = r\mathbf{B}(\beta)\mathbf{E}(\varepsilon)\mathbf{u}_x \tag{4}$$

with the unit vector $\mathbf{u}_x = [1, 0, 0]^T$. Differentiation of (1) with respect to time and ordering of terms yields the velocity

$$\mathbf{v} = \begin{bmatrix} v_x \\ v_y \\ v_z \end{bmatrix} = \begin{bmatrix} \dot{x} \\ \dot{y} \\ \dot{z} \end{bmatrix} = r\mathbf{B}(\beta)\mathbf{E}(\varepsilon) \begin{bmatrix} \dot{r}/r \\ \omega \\ \dot{\varepsilon} \end{bmatrix} \tag{5}$$

with the projected bearing rate

$$\omega = \dot{\beta}\cos\varepsilon \tag{6}$$

Log-spherical coordinates use as state variables, in addition to the angles β and ε, the logarithmic range

$$\varrho = \log(r/R) \;\Rightarrow\; \dot{\varrho} = \dot{r}/r \tag{7}$$

with some normalizing range R as well as the three rate components $\dot{\varrho}$, ω, and $\dot{\varepsilon}$. Denote with subscript 0 all quantities at some given time t_0 and with subscript 1 all at some time $t_1 = t_0 + T$. For brevity, we will further write

$$\mathbf{q} = [\ \varrho,\ \beta,\ \varepsilon\ ]^T \quad \text{and} \quad \dot{\mathbf{q}} = [\ \dot{\varrho},\ \omega,\ \dot{\varepsilon}\ ]^T \tag{8}$$

—with respect to its second component, $\dot{\mathbf{q}}$ is not really the time derivative of $\mathbf{q}$, so we abused notation here a bit for reasons of convenience—in our derivations. Starting from the equations

$$\mathbf{p}_1 = \mathbf{p}_0 + T\mathbf{v}_0 \quad \text{and} \quad \mathbf{v}_1 = \mathbf{v}_0 \tag{9}$$

and in view of

$$\beta_1 = \beta_0 + \beta_{10} \Rightarrow \mathbf{B}(\beta_1) = \mathbf{B}(\beta_0)\mathbf{B}(\beta_{10}) \tag{10}$$

with $\beta_{10} = \beta_1 - \beta_0$ one obtains in combination with eqs. (4) and (5) the propagation correspondence

$$r_1\mathbf{B}_{10}\mathbf{E}_1\mathbf{u}_x = r_0\gamma_{10} \;\; \text{with} \;\; \gamma_{10} = \mathbf{E}_0(\mathbf{u}_x + T\dot{\mathbf{q}}_0) \tag{11}$$

when using the short-hand notation $\mathbf{E}_0 = \mathbf{E}(\varepsilon_0)$, $\mathbf{E}_1 = \mathbf{E}(\varepsilon_1)$, and $\mathbf{B}_{10} = \mathbf{B}(\beta_{10})$. From that, there follows both

$$r_1 = \|\gamma_{10}\|\, r_0 \quad \Longleftrightarrow \quad \varrho_1 = \varrho_0 + \log(\|\gamma_{10}\|) \tag{12}$$

$$\|\gamma_{10}\| = \sqrt{(1 + \dot{\varrho}_0 T)^2 + (\omega_0 T)^2 + (\dot{\varepsilon}_0 T)^2} \tag{13}$$

as well as—the singularity for $\|\gamma_{10}\| = 0$ and for $\|\sigma_{10}\| = 0$ is excepted from further discussion—

$$\cos(\beta_{10}) = X_{10}/\|\sigma_{10}\| \quad \text{and} \quad \sin(\beta_{10}) = Y_{10}/\|\sigma_{10}\| \tag{14}$$

$$\sin(\varepsilon_1) = Z_{10}/\|\gamma_{10}\| \quad \Rightarrow \quad \cos(\varepsilon_1) = \|\sigma_{10}\|/\|\gamma_{10}\| \tag{15}$$

$$\gamma_{10} = [\ X_{10}, Y_{10}, Z_{10}\ ]^T \quad \text{and} \quad \sigma_{10} = [\ X_{10}, Y_{10}, 0\ ]^T \tag{16}$$

The state propagation of the rates is obtained from eqs. (5) and (10) in combination with the identity $\mathbf{v}_1 = \mathbf{v}_0$ yielding

$$\dot{\mathbf{q}}_1 = \frac{1}{\|\gamma_{10}\|}\mathbf{E}_1^T\ \mathbf{B}_{10}^T\mathbf{E}_0\dot{\mathbf{q}}_0 \tag{17}$$

which can be shown (cf. [8] for the details) to imply

$$T\dot{\varrho}_1 = 1 - \frac{1 + \dot{\varrho}_0 T}{\|\gamma_{10}\|^2} \tag{18}$$

The use of log-spherical coordinates hence produces additive increments for both log-range and bearing. It is a known decisive feature that these *increments as well as all other propagation equations depend neither on the range nor on the bearing of the tracked object*, but only on the last four components ε, $\dot{\varrho}$, ω, and $\dot{\varepsilon}$ of its state. In addition, the *propagation equation of the normalized range rate $\dot{\varrho} = \dot{r}/r$ does not depend on elevation*.

The undisturbed straight line relative movement of the tracked object uniquely determines a plane with normal vector

$$\mathbf{n} = \frac{\mathbf{p}_0 \times \mathbf{v}_0}{\|\mathbf{p}_0 \times \mathbf{v}_0\|} \tag{19}$$

—in case the tracked object is permanently moving directly towards the platform (or exactly in the opposite direction), the plane is not uniquely defined, but, of course, there are still vectors $\mathbf{n}$ normal to the movement—and going through the initial origin of the platform-oriented coordinate system. If $\tilde{\varrho}$, $\tilde{\beta}$, $\tilde{\varepsilon}$, $\dot{\tilde{\varrho}}$, $\tilde{\omega}$, and $\dot{\tilde{\varepsilon}}$ denote the quantities of the state vector with respect to a rotated coordinate system whose z-axis is co-aligned with $\mathbf{n}$, then (relative) elevation $\tilde{\varepsilon}$ and (relative) elevation rate $\dot{\tilde{\varepsilon}}$ will be zero throughout, while (logarithmic) range and normalized range rate are not affected by the rotation of the coordinate system. A formal replacement of each variable $*$ by $\tilde{*}$ in eqs. (11) to (18) while honoring $\tilde{\varepsilon} = 0$ and $\dot{\tilde{\varepsilon}} = 0$ leads to the two-dimensional log-polar propagation equations in the variables $\tilde{\varrho} = \varrho$, $\tilde{\beta}$, $\dot{\tilde{\varrho}} = \dot{\varrho}$, and $\tilde{\omega}$. As we have $\dot{\tilde{\varepsilon}} = 0$, there always holds

$$\omega = \tilde{\omega}\cos(\vartheta) \quad \text{and} \quad \dot{\varepsilon} = \tilde{\omega}\sin(\vartheta) \tag{20}$$

with

$$|\tilde{\omega}| = \sqrt{\omega^2 + \dot{\varepsilon}^2} \tag{21}$$

and some angle ϑ. With all of this, the conservation law of the angular momentum reads

$$\tilde{\omega}_1 = \frac{1}{\|\gamma_{10}\|^2}\,\tilde{\omega}_0 = \frac{r_0^2}{r_1^2}\,\tilde{\omega}_0 \tag{22}$$

which shows that also the *propagation equation of the effective bearing rate $\tilde{\omega}$ does not depend on elevation*.

III. Log-Spherical EKF: Prediction and Update

In order to implement a recursive state estimator in log-spherical coordinates, an extended Kalman filter is set up. For such a filter, an update with bearing and elevation is trivial as these are direct measurements of state variables. Propagation is more involved as the state transition equations are non-linear in the states. The computation of the corresponding Jacobians is somewhat tedious and has been elaborated in [8]. However, it is in fact not necessary to implement those. Instead, one can convert the log-spherical state and covariance into Cartesian ones (the corresponding Jacobians look much simpler and can also be found in [8] and elsewhere), perform the prediction there, and transform back into log-spherical coordinates immediately before update. Independently of the chosen (unknown) range for the transformation (e. g., the one from the prior derived later on), the result is *exactly the same as with the direct log-spherical implementation* as long as there is no process noise. And, a physically meaningful process noise is more easily added in Cartesian than in log-spherical space although then the initially assumed range has an influence on the result and thus must be chosen reasonably in order to get coherent (although most likely not correct) range estimates in due course. Typically, a white acceleration Cartesian process noise covariance

$$\mathbf{Q}_1 = \begin{bmatrix} \mathbf{D}T^3/3 & \mathbf{D}T^2/2 \\ \mathbf{D}T^2/2 & \mathbf{D}T \end{bmatrix} \tag{23}$$

is assumed with $\mathbf{D}$ being the diagonal matrix of noise levels q_{xy}, q_{xy}, and q_z.

IV. EKF: Initialization

With prediction and update of our EKF being stated, we are ready to discuss the two different ways of initializing it.

A. Prior for log-range and log-spherical rates

With initially measured bearing and elevation and using them unalteredly (including the corresponding measurement error variances) to initialize the respective angular states of our filter, we seek initial estimates (expected values as well as covariances) for the remaining states. We assume that the sensor has some minimum and maximum detection range r_{min} and r_{max}. Then, an assumed diffuse prior after detection becomes a homogeneous density $p(x, y, z)$ on a spherical shell yielding

$$p(r) = p_0 r^2 = \frac{r^2}{\frac{1}{3}(r_{\text{max}}^3 - r_{\text{min}}^3)} \quad \text{for} \quad r_{\text{min}} \le r \le r_{\text{max}} \tag{24}$$

and $p(r) = 0$ elsewhere.

With this, we find for the logarithmic range an expected value

$$\begin{aligned} \bar{\varrho} = \mathrm{E}[\varrho] &= p_0 \int_{r_{\text{min}}}^{r_{\text{max}}} \log(r/R) r^2 \, \mathrm{d}r \\ &= \frac{1}{3} p_0 \left[r^3 \left(\log(r/R) - \frac{1}{3} \right) \right]_{r_{\text{min}}}^{r_{\text{max}}} \\ &= \frac{r_{\text{max}}^3 \varrho_{\text{max}} - r_{\text{min}}^3 \varrho_{\text{min}}}{r_{\text{max}}^3 - r_{\text{min}}^3} - \frac{1}{3} \end{aligned} \tag{25}$$

with

$$\varrho_{\text{min}} = \log(r_{\text{min}}/R) \quad \text{and} \quad \varrho_{\text{max}} = \log(r_{\text{max}}/R) \tag{26}$$

as well as an expected squared value

$$\begin{aligned} \mathrm{E}\left[\varrho^2\right] &= p_0 \int_{r_{\text{min}}}^{r_{\text{max}}} \log^2(r/R) r^2 \, \mathrm{d}r \\ &= \frac{1}{3} p_0 \left[r^3 \left(\log^2(r/R) - \frac{2}{3}\log(r/R) + \frac{2}{9} \right) \right]_{r_{\text{min}}}^{r_{\text{max}}} \\ &= \frac{r_{\text{max}}^3 \left(\varrho_{\text{max}}^2 - \frac{2}{3}\varrho_{\text{max}}\right) - r_{\text{min}}^3 \left(\varrho_{\text{min}}^2 - \frac{2}{3}\varrho_{\text{min}}\right)}{r_{\text{max}}^3 - r_{\text{min}}^3} + \frac{2}{9} \end{aligned} \tag{27}$$

from which the variance can be computed to be

$$\mathrm{Var}[\varrho] = \mathrm{E}\left[\varrho^2\right] - \bar{\varrho}^2 = \frac{1}{9} - \frac{r_{\text{max}}^3 r_{\text{min}}^3 (\varrho_{\text{max}} - \varrho_{\text{min}})^2}{(r_{\text{max}}^3 - r_{\text{min}}^3)^2} \tag{28}$$

In the limit of zero minimum detection range, the results obtained simplify to

$$\mathrm{E}[\varrho] = \varrho_{\text{max}} - \frac{1}{3} \quad \text{and} \quad \mathrm{Var}[\varrho] = \frac{1}{9} \tag{29}$$

which in particular means that the filter is then initialized with slightly more than half the maximum detection range according to $r_{\text{initial}} = \exp(-1/3) r_{\text{max}} \approx 0.53 r_{\text{max}}$.

In order to derive corresponding expressions for the log-spherical rates, we first investigate the simplified case of a fixed platform. We choose an isotropic prior in the Cartesian velocity with zero mean and independent of position, i. e., we assume, in particular, $\mathrm{E}[\dot{x}] = \mathrm{E}[\dot{y}] = \mathrm{E}[\dot{z}] = 0$ as well as $\mathrm{Var}[\dot{x}] = \mathrm{Var}[\dot{y}] = \mathrm{Var}[\dot{z}] = \sigma_{\text{vel}}^2$ to hold. From

$$\dot{\varrho} = \frac{\dot{r}}{r} = \frac{x\dot{x} + y\dot{y} + z\dot{z}}{r^2} \tag{30}$$

we get

$$\mathrm{E}[\dot{\varrho}] = \mathrm{E}\left[\frac{x}{r^2}\right] \underbrace{\mathrm{E}[\dot{x}]}_{=0} + \mathrm{E}\left[\frac{y}{r^2}\right] \underbrace{\mathrm{E}[\dot{y}]}_{=0} + \mathrm{E}\left[\frac{z}{r^2}\right] \underbrace{\mathrm{E}[\dot{z}]}_{=0} = 0 \tag{31}$$

and next

$$\begin{aligned} \mathrm{E}\left[\dot{\varrho}^2\right] &= \mathrm{E}\left[\frac{x^2}{r^4}\right] \mathrm{E}\left[\dot{x}^2\right] + 2\,\mathrm{E}\left[\frac{xy}{r^4}\right] \underbrace{\mathrm{E}[\dot{x}\dot{y}]}_{=0} \\ &\quad + \mathrm{E}\left[\frac{y^2}{r^4}\right] \mathrm{E}\left[\dot{y}^2\right] + 2\,\mathrm{E}\left[\frac{yz}{r^4}\right] \underbrace{\mathrm{E}[\dot{y}\dot{z}]}_{=0} \\ &\quad + \mathrm{E}\left[\frac{z^2}{r^4}\right] \mathrm{E}\left[\dot{z}^2\right] + 2\,\mathrm{E}\left[\frac{zx}{r^4}\right] \underbrace{\mathrm{E}[\dot{z}\dot{x}]}_{=0} \\ &= \mathrm{E}\left[\frac{x^2 + y^2 + z^2}{r^4}\right] \sigma_{\text{vel}}^2 = \mathrm{E}\left[\frac{1}{r^2}\right] \sigma_{\text{vel}}^2 \end{aligned} \tag{32}$$

As there holds

$$\mathrm{E}\left[\frac{1}{r^2}\right] = p_0 \int_{r_{\text{min}}}^{r_{\text{max}}} \frac{1}{r^2} r^2 \, \mathrm{d}r = 3 \frac{r_{\text{max}} - r_{\text{min}}}{r_{\text{max}}^3 - r_{\text{min}}^3} \tag{33}$$

the variance of the normalized range rate reads

$$\mathrm{Var}[\dot{\varrho}] = 3\sigma_{\text{vel}}^2 \frac{r_{\text{max}} - r_{\text{min}}}{r_{\text{max}}^3 - r_{\text{min}}^3} = \frac{3\sigma_{\text{vel}}^2}{r_{\text{max}}^2 + r_{\text{max}} r_{\text{min}} + r_{\text{min}}^2} \tag{34}$$

which reduces in the limit of zero detection range to

$$\mathrm{Var}[\dot{\varrho}] = \frac{3\sigma_{\text{vel}}^2}{r_{\text{max}}^2} \tag{35}$$

Now, we compute the still missing cross-covariance between log-spherical range and range-rate component. Not surprisingly, the correlation is zero which is confirmed by looking at

$$\begin{aligned} \mathrm{E}[(\varrho - \bar{\varrho})\,\dot{\varrho}] &= \mathrm{E}[\varrho\dot{\varrho}] - \bar{\varrho} \underbrace{\mathrm{E}[\dot{\varrho}]}_{=0} = \mathrm{E}\left[\frac{\varrho x}{r^2}\right] \underbrace{\mathrm{E}[\dot{x}]}_{=0} \\ &\quad + \mathrm{E}\left[\frac{\varrho y}{r^2}\right] \underbrace{\mathrm{E}[\dot{y}]}_{=0} + \mathrm{E}\left[\frac{\varrho z}{r^2}\right] \underbrace{\mathrm{E}[\dot{z}]}_{=0} = 0 \end{aligned} \tag{36}$$

We conclude the fixed-platform case by looking at the remaining rates. For them, we use the conjecture—the proof for preconditions and correctness of that conjecture is still open—that the isotropic Cartesian velocity prior implies an also isotropic log-spherical rates prior, so that initialization with zero mean and a variance value as computed in eq. (34) also for both ω and $\dot{\varepsilon}$ (without correlation between them or to any of the other states) would be the right approach.

While we were able to derive prior expressions for fixed platforms with a certain level of rigorousness, the extension to the case of moving platforms is by no means trivial when it comes to the computation of the log-spherical rates prior. Therein, one would have to distinguish clearly between the velocities relative to the platform—those relative velocities are the ones to be converted to and from log-spherical space in order to get the desired decoupling of the remaining components from the range—and velocities in a stationary coordinate system that happens to have its origin in the current platform position. It is for the latter that the assumption of zero mean and isotropic covariance in Cartesian velocity makes sense, not for the former one. Unfortunately, there appears to be no way of maintaining the principles used to derive our results in a rigorous fashion in this case. So, we resort to a heuristic approach here. Based on the measured pair of bearing $\beta_{\mathrm{m},0}$ and elevation $\varepsilon_{\mathrm{m},0}$ and starting from a known platform velocity $\mathbf{v}_{\text{own}}$ and an assumed prior object velocity $\mathbf{v}_{\text{abs},0} = \mathbf{0}$ being translated into the prior relative velocity $\mathbf{v}_0 = \mathbf{v}_{\text{abs},0} - \mathbf{v}_{\text{own}} = -\mathbf{v}_{\text{own}}$, we use the prior range $r_{\text{initial}} = R\exp(\bar{\varrho})$ and eq. (5) to initialize the rate components via

$$\begin{bmatrix} \dot{\varrho}_0 \\ \omega_0 \\ \dot{\varepsilon}_0 \end{bmatrix} = -\mathbf{E}^T(\varepsilon_{\mathrm{m},0})\mathbf{B}^T(\beta_{\mathrm{m},0})\frac{\mathbf{v}_{\text{own}}}{r_{\text{initial}}} \tag{37}$$

Covariances are initialized as if the platform were not moving. Herewith, we ignore existing correlations within our initial estimates that certainly exist as we, in particular, use the same measured values for initialization of both angles and rates. However, an investigation of how those correlations can be quantified is left to future research.

B. Batch estimator

As an alternative to a one-point initialization, we seek for a batch estimate of all observable states based on several measurement pairs. We note that an exact solution (that would be in analogy to the two-point differencing for Cartesian-complete measurements) does not exist, as we need at least three measurement pairs (yielding six equations) for the five quantities to estimate. Based on the measured values $\beta_{\mathrm{m},i}$ and $\varepsilon_{\mathrm{m},i}$ at times t_i, we search for optimum values β_0, ε_0, $\dot{\varrho}_0$, ω_0, and $\dot{\varepsilon}_0$. But, the minimization of

$$\sum_i \left(\frac{(\beta_{\mathrm{m},i} - \beta_i)^2}{\sigma_\beta^2} + \frac{(\varepsilon_{\mathrm{m},i} - \varepsilon_i)^2}{\sigma_\varepsilon^2} \right) \tag{38a}$$

for a straight line constant velocity movement with

$$\begin{aligned} \beta_i &= \beta(\beta_0, \varepsilon_0, \dot{\varrho}_0, \omega_0, \dot{\varepsilon}_0, T_i) \\ \varepsilon_i &= \varepsilon(\beta_0, \varepsilon_0, \dot{\varrho}_0, \omega_0, \dot{\varepsilon}_0, T_i) \end{aligned} \tag{38b}$$

and $T_i = t_i - t_0$ states a non-linear *least-squares* (LS) problem without closed form solution. As an approximate solution, we propose to first determine an estimate of the normal vector $\mathbf{n}$ of eq. (19) and then solve, in an LS sense, the set of equations resulting from the propagation equation (16) in the plane specified by $\mathbf{n}$.

For the true states, there holds

$$\mathbf{n}^T\mathbf{w}_i = 0 \quad \text{for} \quad \mathbf{w}_i = \begin{bmatrix} \cos(\varepsilon_i)\cos(\beta_i) \\ \cos(\varepsilon_i)\sin(\beta_i) \\ \sin(\varepsilon_i) \end{bmatrix} \tag{39}$$

We obtain the estimate of $\mathbf{n}$ from the measured unit vectors $\mathbf{w}_{\mathrm{m},i}$ by selecting it to yield, under the constraint $\|\mathbf{n}\| = 1$,

$$\min_{\mathbf{n}} \left\{ \sum_i (\mathbf{n}^T\mathbf{w}_{\mathrm{m},i})^2 \right\} = \min_{\mathbf{n}} \left\{ \mathbf{n}^T\mathbf{W}\mathbf{n} \right\} \tag{40}$$

with

$$\mathbf{W} := \sum_i \mathbf{w}_{\mathrm{m},i}\mathbf{w}_{\mathrm{m},i}^T \tag{41}$$

Consequently, $\mathbf{n}$ is chosen as an unimodular eigenvector referring to the smallest eigenvalue of $\mathbf{W}$.

With this $\mathbf{n}$ written as

$$\mathbf{n} = \begin{bmatrix} n_x \\ n_y \\ n_z \end{bmatrix} = \begin{bmatrix} \cos(\bar{\beta})\cos(\bar{\varepsilon}) \\ \sin(\bar{\beta})\cos(\bar{\varepsilon}) \\ \sin(\bar{\varepsilon}) \end{bmatrix} \tag{42}$$

the transformation matrix

$$\mathbf{R} = \begin{bmatrix} -\cos(\bar{\beta})\sin(\bar{\varepsilon}) & -\sin(\bar{\beta}) & \cos(\bar{\beta})\cos(\bar{\varepsilon}) \\ -\sin(\bar{\beta})\sin(\bar{\varepsilon}) & \cos(\bar{\beta}) & \sin(\bar{\beta})\cos(\bar{\varepsilon}) \\ \cos(\bar{\varepsilon}) & 0 & \sin(\bar{\varepsilon}) \end{bmatrix} \tag{43}$$

is used to compute transformed values according to

$$\tilde{\mathbf{w}}_{\mathrm{m},i} = \mathbf{R}^T\mathbf{w}_{\mathrm{m},i} \tag{44}$$

where, for an $\mathbf{R}$ without error, the vectors $\tilde{\mathbf{w}}_i = \mathbf{R}^T\mathbf{w}_i$ would have zero z-components and could thus be written as

$$\tilde{\mathbf{w}}_i = \begin{bmatrix} \cos(\tilde{\beta}_i) \\ \sin(\tilde{\beta}_i) \\ 0 \end{bmatrix} \tag{45}$$

For the so defined transformed bearings $\tilde{\beta}_i$ in the tilted plane, eq. (16) implies

$$\sin(\tilde{\beta}_i - \tilde{\beta}_0)(1 + \dot{\varrho}_0 T_i) - \cos(\tilde{\beta}_i - \tilde{\beta}_0)\tilde{\omega}_0 T_i = 0 \tag{46}$$

that can, with the abbreviations

$$c_i = \cos(\tilde{\beta}_i) \quad \text{and} \quad s_i = \sin(\tilde{\beta}_i) \tag{47}$$

$$\mathbf{m}_i^T = [s_i, -c_i, s_iT_i, -c_iT_i, -c_iT_i, -s_iT_i] \tag{48}$$

$$\mathbf{t}^T = [c_0, s_0, c_0\dot{\varrho}_0, s_0\dot{\varrho}_0, c_0\tilde{\omega}_0, s_0\tilde{\omega}_0] \tag{49}$$

be written as

$$\mathbf{t}^T\mathbf{m}_i = 0 \tag{50}$$

Moreover, there must hold

$$\mathbf{t}^T\mathbf{m} = 1 \quad \text{with} \quad \mathbf{m}^T = [c_0, s_0, 0, 0, 0, 0] \tag{51}$$

With this result, we use the measured vectors $\mathbf{m}_{\text{m},i}$ and $\mathbf{m}_\text{m}$ and try to determine $\mathbf{t}$ via

$$\min_{\mathbf{t}} \Big\{ \sum_i (\mathbf{t}^T \mathbf{m}_{\text{m},i})^2 + (\mathbf{t}^T \mathbf{m}_\text{m} - 1)^2 \Big\} \tag{52}$$

or, equivalently,

$$\min_{\mathbf{t}} \Big\{ \mathbf{t}^T \mathbf{M} \mathbf{t} - 2\mathbf{t}^T \mathbf{m}_\text{m} + 1 \Big\} \tag{53}$$

with

$$\mathbf{M} := \mathbf{m}_\text{m} \mathbf{m}_\text{m}^T + \sum_i \mathbf{m}_{\text{m},i} \mathbf{m}_{\text{m},i}^T \tag{54}$$

under the constraint $c_0^2 + s_0^2 = 1$ and honoring the special structure of $\mathbf{t}$ given in eq. (49).

In order to determine the constrained optimum, we mimimize the Lagrange function

$$L(\lambda) := \mathbf{t}^T \mathbf{M} \mathbf{t} - 2\mathbf{t}^T \mathbf{m}_\text{m} + \lambda(1 - (c_0^2 + s_0^2)) \tag{55}$$

with multiplier λ with respect to c_0, s_0, $\dot{\varrho}_0$, and $\tilde{\omega}_0$ (and λ which of course just yields the constraint). Derivates can compactly be written by using further abbreviations

$$\mathbf{a}^T = [c_0, s_0], \quad \mathbf{a}_\text{m}^T = [c_{\text{m},0}, s_{\text{m},0}] \tag{56}$$

and

$$\mathbf{A}^T = \begin{bmatrix} 1 & 0 & \dot{\varrho}_0 & 0 & \tilde{\omega}_0 & 0 \\ 0 & 1 & 0 & \dot{\varrho}_0 & 0 & \tilde{\omega}_0 \end{bmatrix} \tag{57}$$

With $\mathbf{0}$ being a 2×1 vector with zero elements, we can write

$$\mathbf{t} = \begin{bmatrix} \mathbf{a} & \mathbf{0} & \mathbf{0} \\ \mathbf{0} & \mathbf{a} & \mathbf{0} \\ \mathbf{0} & \mathbf{0} & \mathbf{a} \end{bmatrix} \begin{bmatrix} 1 \\ \dot{\varrho}_0 \\ \tilde{\omega}_0 \end{bmatrix} = \mathbf{A}\mathbf{a} \tag{58}$$

For the derivatives, we find

$$0 \stackrel{!}{=} \frac{1}{2} \frac{\partial L}{\partial \left[\dot{\varrho}_0, \tilde{\omega}_0\right]^T} = \begin{bmatrix} \mathbf{0}^T & \mathbf{a}^T & \mathbf{0}^T \\ \mathbf{0}^T & \mathbf{0}^T & \mathbf{a}^T \end{bmatrix} \mathbf{M}\mathbf{t} \tag{59}$$

and

$$0 \stackrel{!}{=} \frac{1}{2} \frac{\partial L}{\partial \mathbf{a}} = \mathbf{A}^T \mathbf{M} \mathbf{t} - \lambda \mathbf{a} - \mathbf{a}_\text{m} \tag{60}$$

Still, a closed-form solution of this resulting set of polynomial equation is, if at all, hard to find. However, we can determine the pair $\dot{\varrho}_0$ and $\tilde{\omega}_0$ as a function of $\mathbf{a}$ and vice versa and, with this, are able to set up an iterative scheme. By writing in a block-wise fashion

$$\mathbf{M} = \begin{bmatrix} \mathbf{M}_{11} & \mathbf{M}_{12} & \mathbf{M}_{13} \\ \mathbf{M}_{12}^T & \mathbf{M}_{22} & \mathbf{M}_{23} \\ \mathbf{M}_{13}^T & \mathbf{M}_{23}^T & \mathbf{M}_{33} \end{bmatrix} \tag{61}$$

eq. (59) becomes

$$\begin{bmatrix} \mathbf{a}^T \mathbf{M}_{12}^T \mathbf{a} & \mathbf{a}^T \mathbf{M}_{22} \mathbf{a} & \mathbf{a}^T \mathbf{M}_{23} \mathbf{a} \\ \mathbf{a}^T \mathbf{M}_{13}^T \mathbf{a} & \mathbf{a}^T \mathbf{M}_{23}^T \mathbf{a} & \mathbf{a}^T \mathbf{M}_{33} \mathbf{a} \end{bmatrix} \begin{bmatrix} 1 \\ \dot{\varrho}_0 \\ \tilde{\omega}_0 \end{bmatrix} = \mathbf{0} \tag{62}$$

which delivers $\dot{\varrho}_0$ and $\tilde{\omega}_0$ for a given $\mathbf{a}$. On the other hand, eq. (60) is equivalent to

$$\mathbf{a} = -(\lambda \mathbf{1} - \mathbf{A}^T \mathbf{M} \mathbf{A})^{-1} \mathbf{a}_\text{m} \tag{63}$$

Computation of the inverse as quotient of adjoint and determinant plus successive insertion into the constraint $\mathbf{a}^T \mathbf{a} = 1$ yields a fourth-order polynomial in the multiplier λ. Once among the real toots of the polynomial that one minimizing $L(\lambda)$ has been determined (for given $\dot{\varrho}_0$ and $\tilde{\omega}_0$), $\mathbf{a}$ is known, too.

With the equations above, $\mathbf{a}$ can be, starting from initial value $\mathbf{a}_\text{m}$, determined as fixed point of the mentioned iterative scheme. Convergence appears to be quite fast and can, if necessary, be accelerated by commonly known methods.

With estimates c_0 and s_0 as well as $\dot{\varrho}_0$ and $\tilde{\omega}_0$ now obtained, we have to transform back from the tilted plane. The angles β_0 and ε_0 are obtained from the vector

$$\frac{\mathbf{p}_0}{r_0} = \begin{bmatrix} \cos(\beta_0)\cos(\varepsilon_0) \\ \sin(\beta_0)\cos(\varepsilon_0) \\ \sin(\varepsilon_0) \end{bmatrix} = \mathbf{R} \begin{bmatrix} c_0 \\ s_0 \\ 0 \end{bmatrix} \tag{64}$$

while the rates are computed via

$$\frac{\mathbf{v}_0}{r_0} = \mathbf{R} \begin{bmatrix} c_0 \dot{\varrho}_0 - s_0 \tilde{\omega}_0 \\ s_0 \dot{\varrho}_0 + c_0 \tilde{\omega}_0 \\ 0 \end{bmatrix} \tag{65}$$

and finally as

$$\dot{\mathbf{q}}_0 = \mathbf{E}^T(\varepsilon_0) \mathbf{B}^T(\beta_0) \frac{\mathbf{v}_0}{r_0} \tag{66}$$

We are unable to derive explicit expressions for the expected squared estimation error of the proposed batch estimator. One first guess would be to use the *Cramer-Rao lower bound* (CLRB) of the upcoming section, evaluated at the estimates instead of the (unknown) true object state. The simulation results therein suggest that this approach can be considered appropriate at least to a certain extent although a more rigorous investigation of this aspect is required in the future.

V. Simulation Results

In order to get some insight into the estimation performance achievable with an EKF using the derived prior and with the proposed batch estimator, we have simulated two different scenarios with tracked objects performing noise-free constant velocity motions. In both cases, a sensor receiving angular measurements with sample time $T = 1\,\text{s}$ and accuracies $\sigma_\beta = \sigma_\varepsilon = 0.2\,\text{deg}$ was assumed to be mounted on a platform starting from initial position zero and moving horizontally in pure x-direction with speed $v_\text{own} = 200\,\text{m/s}$. Initial position and velocity of the object to be tracked were $\mathbf{p}_0^T = [15500, -11500, 1250]\,\text{m}$ with $\mathbf{v}_0^T = [-50, 50, 25]\,\text{m/s}$ for the first considered case and $\mathbf{p}_0^T = [13250, 350, 180]\,\text{m}$ with $\mathbf{v}_0^T = [-75, 5, 2]\,\text{m/s}$ for the second one. Herewith, the tracked object was basically on a passing course in the first scenario, while its course was close to collision in the second. We ran the described extended Kalman filter (assuming some small process noise $q_{xy} = q_z = 10\,\text{m}^2/\text{s}^3$ for it) initialized with the derived prior (for $r_\text{min} = 0\,\text{m}$, $r_\text{max} = 25\,\text{km}$, and $\sigma_\text{vel} = 500\,\text{m/s}$) and investigated the *root mean square error* (RMSE) obtained with it for the five observable states in $M = 1000$ Monte-Carlo runs. For comparison, we also ran a standard Cartesian-state EKF using Jacobians in the covariance update. The position component of the state was initialized by transforming a polar measurement with its range being half the maximum detection range in combination with the measured bearing and elevation according to eq. (1). The corresponding covariance was chosen to be $\mathbf{B}(\beta)\mathbf{E}(\varepsilon)\mathbf{C}_0\mathbf{E}^T(\varepsilon)\mathbf{B}^T(\beta)$ where the diagonal matrix $\mathbf{C}_0$ had entries $r_{\max}^2/12$, $r_{\max}^2\sigma_\beta^2/4$, and $r_{\max}^2\sigma_\varepsilon^2/4$. Initial velocity was assumed to be zero with uncorrelated errors of variance σ_{vel}^2 each. We compared the result of both recursive estimators wth the CRLB based on all measurements received up to and including the respective instance of time. This CRLB is the inverse of the *Fisher information matrix* reading, without prior knowledge,

$$\mathbf{I}(t_j) = \sum_{i \le j} \left(\frac{1}{\sigma_\beta^2} \mathbf{b}_{ij} \mathbf{b}_{ij}^T + \frac{1}{\sigma_\varepsilon^2} \mathbf{e}_{ij} \mathbf{e}_{ij}^T \right) \tag{67}$$

with

$$\mathbf{b}_{ij} = \frac{\partial \beta_i}{\partial \mathbf{s}_j},\ \mathbf{e}_{ij} = \frac{\partial \varepsilon_i}{\partial \mathbf{s}_j},\ \mathbf{s}_j = \left[\ \beta_j,\, \varepsilon_j,\, \dot{\varrho}_j,\, \omega_j,\, \dot{\varepsilon}_j\ \right]^T \tag{68}$$

The CRLB constitutes a lower limit on the estimation error covariance any unbiased estimator can achieve.

The performance of the proposed batch estimator was analysed for the very same scenarios. Here, we have limited the length of the batch, i. e., the number of measurement pairs used for computing an estimate, to be six (or accordingly lower as long as the number of received measurement pairs had not reached that value yet). Again, the corresponding CRLB served as a benchmark. Moreover, two other batch estimators using the same up to six measurements were implemented. The first one used separate regressions on bearing and elevation. As the constant linear motion in Cartesian space leads to non-linear movements in those two angular coordinates, a quadratic regression was used, i. e., estimates for β_j and $\dot{\beta}_j$ were obtained from determining, using the measurements $\beta_{\mathrm{m},i}$ in the batch,

$$\min_{\beta_j, \dot{\beta}_j, \ddot{\beta}_j} \sum_i (\beta_j + \dot{\beta}_j(t_i - t_j) + \ddot{\beta}_j(t_i - t_j)^2 - \beta_{\mathrm{m},i})^2 \tag{69}$$

and likewise for ε_j and $\dot{\varepsilon}_j$. Obviously, this quadratic regression estimator does not provide an estimate for $\dot{\varrho} = \dot{r}/r$. Finally, we applied a general-purpose non-linear least-squares estimator numerical trying to solve, at the cost of much higher computational effort than the other estimators, eq. (38a).

Figs. 1 and 2 show the simulation results, namely the true observable states as well as the RMSE values from the Monte-Carlo runs compared with the respective CRLBs. The first two different CRLBs computed according to eq. (67) depend on whether all measurements or only the six most recent ones are considered where the latter case, of course, yields higher values. The third CRLB differs from the first one by honoring, in addition, the information contained in our assumed prior. With this, we computed the corresponding extended Fisher information matrix (with the prior variances as in eqs. (29) and (35) for zero minimum detection range)

$$\tilde{\mathbf{I}}(t_j) = \begin{bmatrix} 0 & \mathbf{0}^T \\ \mathbf{0} & \mathbf{I}(t_j) \end{bmatrix} + 9\mathbf{r}_{0j}\mathbf{r}_{0j}^T + \frac{r_{\max}^2}{3\sigma_{\text{vel}}^2}\mathbf{d}_{0j}\mathbf{d}_{0j}^T \tag{70}$$

with

$$\mathbf{r}_{0j}^T = \begin{bmatrix} \frac{\partial \varrho_0}{\partial \varrho_j} & \left[\frac{\partial \varrho_0}{\partial \mathbf{s}_j}\right]^T \end{bmatrix},\ \mathbf{d}_{0j}^T = \begin{bmatrix} \frac{\partial \dot{\varrho}_0}{\partial \varrho_j} & \left[\frac{\partial \dot{\varrho}_0}{\partial \mathbf{s}_j}\right]^T \end{bmatrix} \tag{71}$$

Among all three CRLB variants, this third one yields the smallest values. It should, however, be clear that our similation setup does not fully match the assumptions behind this third CRLB—we have chosen fixed initial (logarithmic) range and (normalized) range rate and thus do not generate random errors on the corresponding initial estimates—and hence deviations from that are inevitable here. Moreover, when interpreting the CRLB one must not forget that it refers to unbiased estimators only and that a biased estimator may produce, for specific values, a lower RMSE than suggested by the CRLB.

Fig. 1 refers to the almost passing and thus to the less critical case (closest distance about $9.7\,\mathrm{km}$). We note that both recursive estimators, log-spherical and Cartesian EKF, deliver very similar results in this case. They show, after some initial phase, close to CRLB performance for quite some time. Due to the assumed process noise however, they tend to loose some information in the long run and show higher errors than the CRLB then. When comparing the filter results with the CRLB, a closer inspection of the initial phase confirms that the one CRLB honoring the prior (on logarithmic range and normalized range rate) much better matches the filter performance than the one computed based on the angular measurements alone. The match between the CRLB with prior and the actual filter performance is very good indeed, only in the normalized range rate we note some major deviation where we have argued on this behalf already earlier (about the difference between modelling assumption and actually implemented procedure).

Close to CRLB (induced by at most six measurements) performance is also obtained by our batch estimator with small degradations in bearing and normalized range rate. The quadratic regression estimator shows good performance where the assumption of a quadratic pseudo-maneuver in angular space (over the time interval of the measurements incorporated) is fulfilled, here for the bearing (and its rate). It performs less well where this is assumption is less fulfilled, here for the elevation (and in particular its rate). The general-purpose LS estimator performs best in the angles, but shows some deficiency in the rates as long as angular rates are small.

This deficiency appears to be inherent in the general purpose non-linear LS estimator and leads to rate errors that exceed the actual rates by orders of magnitude in the more critical second scenario where the object was closer to collision (closest distance roughly $710\,\mathrm{m}$). Because of those unreasonable rate values delivered by the non-linear LS estimator, we have omitted it from Fig. 2 showing the results for this case. For the other estimators, similar remarks as for the first scenario can be

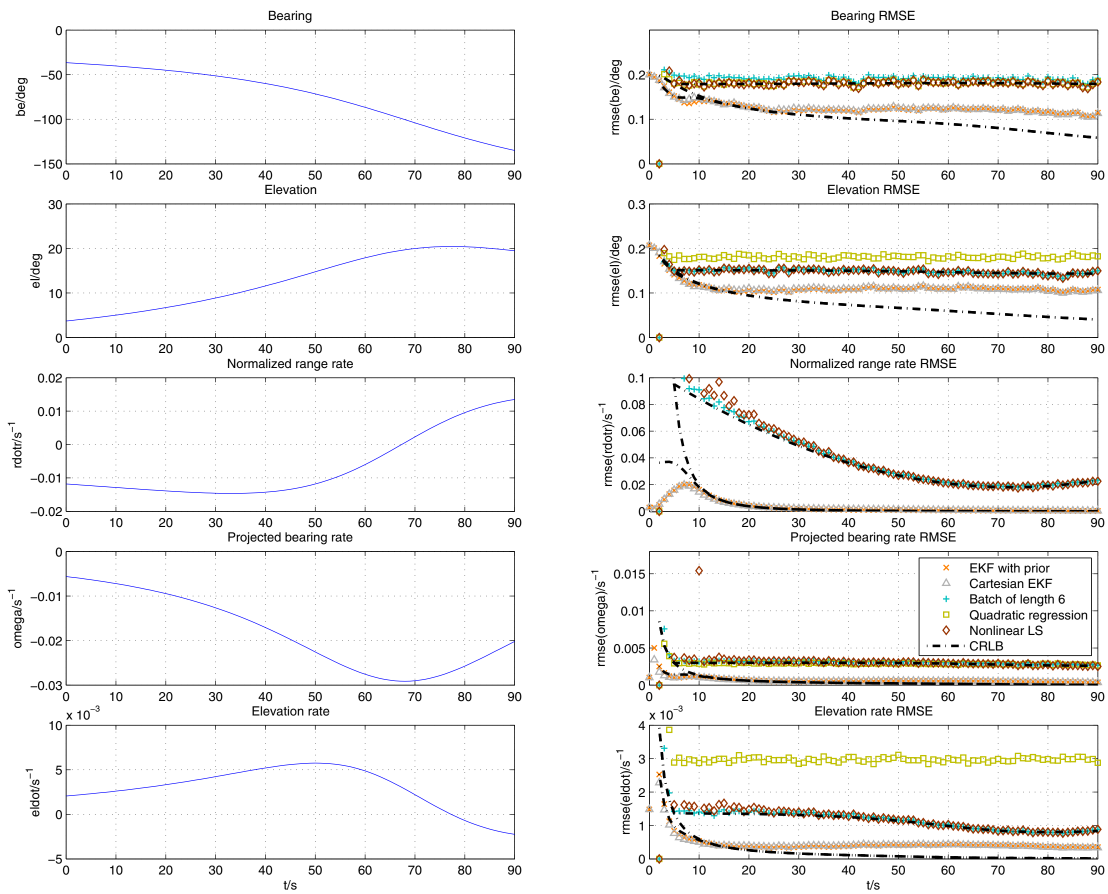

Figure 1. True observable states (left) as well as root mean square errors (right) from 1000 Monte Carlo runs compared with CRLBs for a tracked object on a passing course. Used estimators were a log-spherical EKF initialized with the derived prior, a Cartesian EKF initialized with a converted prior, the proposed batch estimator, an estimator based on quadratic regression, and a general non-linear least-squares.

stated. All estimators, but especially the quadratic regression estimator due to the then violated assumption of close to constant rates, show some performance degradation near the point of closest distance where angles undergo relatively rapid changes and, thus, some degragation is not totally surprising. Farther away from this special point, the batch CRLB for $\dot{\varrho}$ increases rapidly which confirms the low observability of the normalized range rate for an almost colliding course. Nevertheless, our proposed batch estimator then still reaches close to CRLB performance for that quantity as it does for the other observable states most of the times. There is some phase with reduced accuracy in bearing way before the point of closest distance though. What exactly makes the special geometry in this phase less favorable for the estimator remains unclear for now, the CRLB does not suggest such a problem.

We wrap up the discussion of our simulation results by noting that the EKF running in log-spherical coordinates and being initialized via our derived prior tracks the object without significant problems also in this more critical case. Moreover, we note that it is, in comparison with the Cartesian EKF, better capable of handling the weak observability of the normalized range rate prior to the point of closest approach. Also with respect to the projected bearing rate, its performance is slightly better there.

VI. Conclusion

With this publication, we contributed to the wide field of tracking based on angular-only measurements with focus on filter initialization. In order to perform one-point initialization of an EKF running in log-spherical coordinates, we have derived a prior for the logarithmic range and the normalized range rate that is based on a diffuse Cartesian position prior in combination with (minimum and) maximum detection range of the sensor plus a prior of Cartesian velocity having zero mean and some assumed variance. Derivation of the log-spherical prior was rigourous (up to one conjecture still to be proven) for fixed sensors, a heuristic adaptation to moving sensors was proposed. Simulation results confirmed the applicability of the derived priors for two different scenarios. On the way to an alternative regression-based multi-point initialization, we have

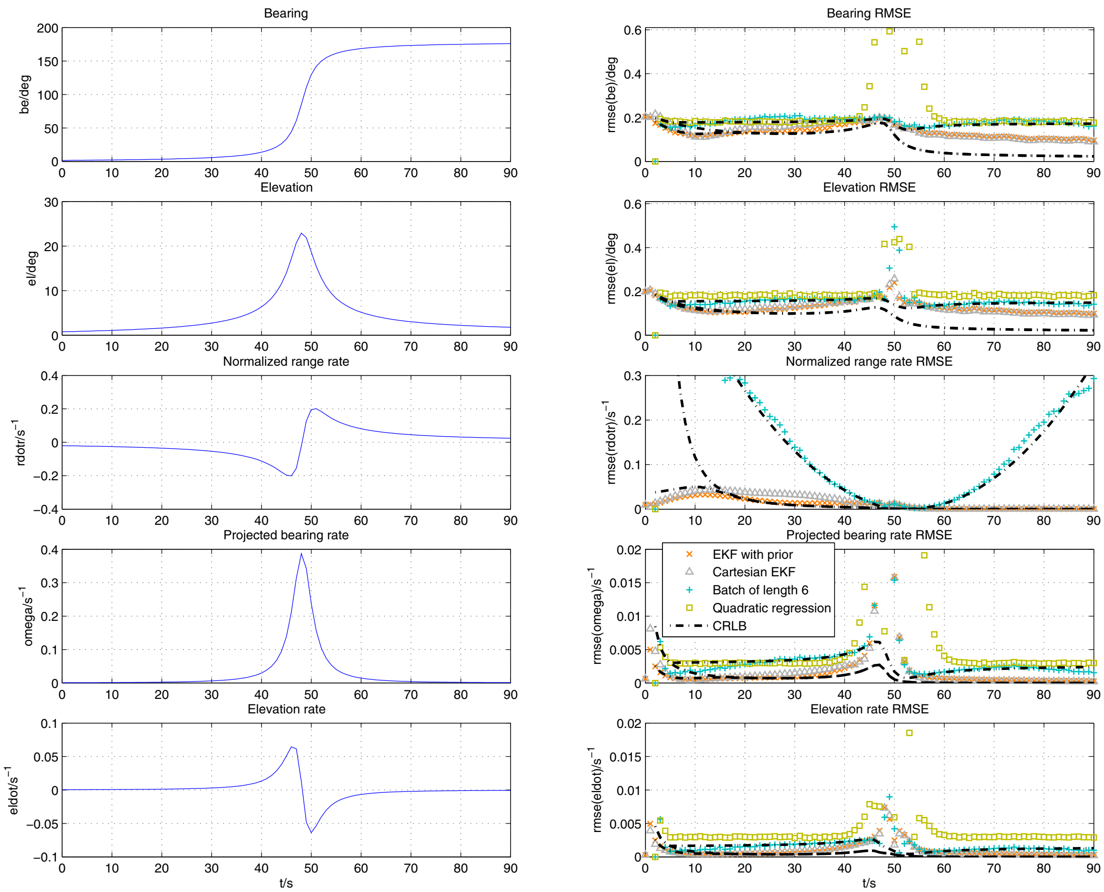

Figure 2. True observable states (left) as well as root mean square errors (right) from 1000 Monte Carlo runs compared with CRLBs for a tracked object on an almost colliding course. Used estimators were a log-spherical EKF initialized with the derived prior, a Cartesian EKF initialized with a converted prior, the proposed batch estimator, and an estimator based on quadratic regression.

proposed a new batch estimator and investigated its (stand-alone without successive filter updates) performance for the same simulated scenarios with promising results.

A more intensive simulation study comparing tracking quality based on one-point vs. multi-point initialization is left for the future, but we expect results in analogy to the ones obtained for Cartesian-complete observations in [12]: Where the assumptions made for the prior reflect reality at least to some extent, its incorporation via the one-point initialization plus successive updates should yield better results than the multi-point initialization not using this valuable information.

References

[1] W. D. Blair, G. A. Watson, T. Kirubarajan, and Y. Bar-Shalom, "Benchmark for radar allocation and tracking in ECM," *IEEE Trans. Aerospace & Electronic Systems*, vol. 34, no. 4, pp. 1097–1114, 1998.

[2] W. Blanding, W. Koch, and U. Nickel, "Tracking through jamming using negative information," in *Proc. ISIF Intern. Conf. on Information Fusion (FUSION)*, 2006, pp. 1–8.

[3] Airborne collision avoidance system (ACAS). Eurocontrol. [Online]. Available: http://www.eurocontrol.int/msa/public/standard_page/ACAS_Startpage.html

[4] Unmanned aircraft systems – ATM collision avoidance requirements. Eurocontrol. [Online]. Available: http://www.eurocontrol.int/msa/gallery/content/public/documents/CAUSE_report_v13.pdf

[5] Mid air collision avoidance system (MIDCAS). [Online]. Available: http://www.midcas.org/

[6] V. Aidala and S. Hammel, "Utilization of modified polar coordinates for bearings-only tracking," *IEEE Trans. Automatic Control*, vol. 28, no. 3, pp. 283–294, 1983.

[7] B. La Scala and M. Morelande, "An analysis of the single sensor bearings-only tracking problem," in *Proc. ISIF Intern. Conf. on Information Fusion (FUSION)*, 2008, pp. 525–530.

[8] D. Fränken and A. Hüpper, "Unified tracking and fusion for airborne collision avoidance using log-polar coordinates," in *Proc. ISIF Intern. Conf. on Information Fusion (FUSION)*, 2012, pp. 1246–1253.

[9] S. J. Julier and J. K. Uhlmann, "Unscented filtering and nonlinear estimation," in *Proceedings of the IEEE*, vol. 92, no. 3, 2004, pp. 401–422.

[10] B. Ristic, S. Arulampalam, and N. Gordon, *Beyond the Kalman Filter*. Artech House, 2004.

[11] Y. Bar-Shalom, "Tracking methods in a multitarget environment," *IEEE Trans. Automatic Control*, vol. 23, no. 4, pp. 618–626, 1978.

[12] M. Mallick and B. La Scala, "Comparison of single-point and two-point difference track initiation algorithms using position measurements," *Acta Automatica Sinica*, vol. 34, no. 3, pp. 258–265, 2008.